HHS Public Access

Author manuscript

Cytoskeleton (Hoboken). Author manuscript; available in PMC 2016 June 30.

Published in final edited form as:

Cytoskeleton (Hoboken). 2015 June ; 72(6): 282–291. doi:10.1002/cm.21227.

Evidence for changes in beta- and gamma-actin proportions during inner ear hair cell life

Leonardo R. Andrade

Laboratory of Cell Structure and Dynamics, National Institute on Deafness and Other Communication Disorders, National Institutes of Health, Bethesda, MD, USA

Abstract

Cytoplasmic actin isoforms beta (β-) and gamma (γ-) perform crucial physiological roles in inner ear hair cells (HC). The stereocilium, which is structured by parallel actin filaments composed of both isoforms, is the responsive organelle to mechanical stimuli such as sound, gravity and head movements. Modifications in isoform proportions affect the function of the stereocilia as previously shown in genetic studies of mutant mice. Here, immunogold labeling TEM studies in mice showed that both β- and γ-actin isoforms colocalize throughout stereocilia actin filaments, adherens junctions and cuticular plates as early as embryonic stage 16.5. Gold-particle quantification indicated that there was 40% more γ- actin than β-actin at E16.5. In contrast, β- and γ-actin were equally concentrated in adult stereocilia of cochlear and vestibular HC. Interestingly, all actin-based structures presented almost five-fold more β-actin than γ-actin in 22 month- old mice, suggesting that γ-actin is probably under-expressed during the aging process. These data provide evidence of dynamic modifications of the actin isoforms in stereocilia, cuticular plates and cell junctions during the whole HC life.

Keywords

β-actin; γ-actin; hair cells; stereocilia; immunogold TEM

Introduction

The actin cytoplasmic isoforms beta (β-) and gamma (γ-) are evolutionarily conserved from primitive organisms to higher vertebrates, yet they differ by only four aminoacid residues in the N-terminus (Vandekerckhove and Weber, 1978). Despite their very slightly molecular differences, the perpetuation of both isoform expressions in a broad range of cells and organisms suggests that they might have distinct functions and concentrations in all actin-based structures (Bergeron et al., 2010; Bunnell and Ervasti, 2011; Dugina et al., 2009). Inner ear hair cells (HCs) rely on actins and accessory proteins to perform their specific functions. Actin filaments form the basic frame of all stereocilia, adherens junctions, cuticular plates, and the lateral wall of outer hair cells (OHCs) (Schwander et al., 2010;

Correspondence to: Av. Carlos Chagas Filho 373, F2-30, ICB, CCS, UFRJ, Ilha do Fundão, Rio de Janeiro, RJ, 21941-902, Brazil. Phone: +55-21-3938-6393. andrade@histo.ufrj.br.

Present address: Laboratory of Biomineralization, Institute of Biomedical Sciences, Health Sciences Center, Federal University of Rio de Janeiro, Rio de Janeiro, RJ, Brazil, 21941-902

Slepecky and Chamberlain, 1985; Tilney et al., 1992; Weaver et al., 1993). Stereocilia are membrane protrusions that are longer than microvilli, arranged in bundles on the apical surface of all HC types, and internally formed by tightly packed, parallel actin filaments. Stereocilia are responsible of detecting mechanical stimuli (sound vibration, gravity and head movements), which are converted into electrical signals transmitted from the inner ear organs to the brain. Mutations in the human β-actin gene (ACTB, location 7p22) cause severe syndromic phenotypes that include deafness and developmental malformations, while mutations in the γ-actin gene (ACTG1, location 17q25) result in dominant non-syndromic progressive hearing loss (DFNA20/26) (Morell et al., 2000; Morín et al., 2009; Procaccio et al., 2006; Rendtorff et al., 2006; van Wijk et al., 2003). These phenotypes indicate that both actin isoforms must be simultaneously expressed in auditory HCs for normal hearing, since one isoform cannot functionally compensate for the other. In mice, ACTB knockout causes embryonic lethality, and although some ACTG1 knockout mice survive, they develop early progressive hearing loss (Belyantseva et al., 2009; Shawlot et al., 1998).

Actin isoform distribution and proportions are not fully known in HCs. Hofer et al. (1997) reported that β-actin was only present in stereocilia while γ-actin localized to stereocilia, cuticular plates, and zonula adherens in chick HCs (ratio of 2γ:1β). Furness et al. (2005) observed β-actin mostly in stereocilia (more concentrated at the periphery), but also at the stereocilia rootlets and the cuticular plate, while γ-actin was found in equal amounts in these structures. At the embryonic stage 16.5 (E16.5), Belyantseva et al. (2009) detected only β-actin in stereocilia from cochlear HCs, whereas γ-actin appeared later in HCs at E18.5. γ-actin was also detected in the stereocilia periphery, and in gaps within the stereocilia core of adult mice subjected to sound damage (Belyantseva et al., 2009). After immunolabeling and γ-actin knockout mouse observations, it was suggested that γ-actin is dispensable for stereocilia formation but is required for their ongoing repair and maintenance (Belyantseva et al., 2009). Perrin et al. (2010) used β- and γ-actin conditional gene ablation technology to show that HC stereocilia development requires at least one cytoplasmic actin, but proceeds normally in the absence of either isoforms. They also found uniform labeling of both isoforms in the inner hair cells (IHC) stereocilia actin cores using dye-labeled preparations of the same primary antibodies, which yielded peripheral localization when relying on secondary antibody labeling (Perrin et al., 2010). These results demonstrate the importance of considering potential artifacts due to steric hindrance in the paracrystalline cores of stereocilia when doing immunolocalization studies.

The actin incorporation and turnover in HC are still a conundrum in the field. Zhang et al. (2012) proposed that actin is replaced only at stereocilia tips, opposing the findings for immature HC published by Schneider et al., (2002) and Rzadzinska et al., (2004), who suggested that actins are continuously incorporated by a treadmilling process from tip to base.

In this paper, immunogold labeling and transmission electron microscopy (TEM) were used to localize and estimate the proportions of β- and γ-actin in actin-based structures of embryonic, post-natal, adult and old mice HCs. The obtained data indicated that HCs might modulate the amounts of actin isoforms in all actin-based structures throughout the cell's lifetime.

Results

Immunofluorescence shows a weak penetration of γ-actin antibody into the actin shaft

Antibody against γ-actin mostly labeled the stereocilia periphery, cuticular plates, apical junctions and microvilli of the supporting cells (Fig. 1). Due to their size, primary antibodies and mainly the secondary antibodies didn't penetrate well into the highly compacted actin core. However, organs of Corti (Figs. 1a and b) and vestibular samples (Figs. 1c-h) presented highly concentrated spots of γ-actin labeling along and at the base of the stereocilia (taper region), possibly caused by mechanical stress during the tissue dissections. The absence of phalloidin labeling in these gaps indicates that the antibodies labeled actin monomers and not actin filaments (Figs. 1c-e).

Immunogold labeling reveals β- and γ-actin as early as E16.5 mouse in all actin-based structures

To better address the actin isoforms' localization in stereocilia, immunogold labeling experiments were performed on ultra-thin sections obtained from the mid-apical turns of E16.5 mouse cochleae. Homogenously distributed gold particles for β- actin and γ-actin were observed in cochlear (Fig. 2a for β-actin and Fig. 2d for γ-actin) and vestibular HC stereocilia (Figs. 2b-c for β-actin) and Figs. 2e-f for γ-actin). Cell junction areas were also positive for both isoforms (Figs. 1a and d). The cuticular plate was not evident at E16.5 in cochlear or utricular hair cells, however, disperse gold particles were noticed in the corresponding areas (Figs. 2a and d). The gold-particles were quantified in cochlear or utricular hair cells and presented in Tables 2 and 3, respectively. In cochlea, γ-actin labeling was higher than β-actin in stereocilia (40%) and junctions (55%), while in the cuticular plate there was no significant difference between the isoforms (Table 2). The same trend also occurred for vestibular hair cells, but with a slight increase of the γ/β ratio (Table 3).

β-and γ-actin seems to be equally present in adult hair cell stereocilia but not in the other studied compartments

Next, the isoform distributions in developing and mature hair cells were studied. Both isoforms colocalized in stereocilia, cuticular plates, and junctions of P4 mouse cochlear HCs (Fig. 3a for β-actin and Figs. 3b-c for γ-actin). Actin labeling was homogeneously distributed along the stereocilia core for both isoforms. Then the actin isoforms in 2-month-old mice (stereocilia are fully grown and matured) were labeled and found in the same distribution pattern as observed in P4 mice (Figs. 3d-f for γ-actin and Figs. 3g-h for β-actin). The immunogold indicated that the isoforms likely copolymerize in the same actin filament. Gold-particle quantification in adult mice indicated equal amounts of γ- and β- in both cochlear and vestibular stereocilia, whereas γ-actin was the preponderant isoform in the cuticular plate and junctions (Tables 2 and 3).

γ-actin was the only isoform detected in the OHC lateral wall adjacent to the plasma membrane of WT mice (SM 1a) and guinea pigs (SM 1b). However, β-actin labeling was observed in γ-actin KO mice (Actg1$^{-/-}$), indicating that γ-actin can be compensated by β-actin in the lateral wall (SM 1c). In this structure, actin and the motor protein prestin are responsible for the OHC electrical motility. γ-actin antibody affinity was also tested for

other animals such as the adult bullfrog (SM 1d) and chick (SM 1e); and presented similar labeling as in the mouse. The antibody against γ-actin proved to be specific, given that no labeling was detected in γ-actin KO mouse sections (SM 1f).

The β- to γ-actin ratio changes considerably in vestibular hair cells of aged mice

ABRs confirmed that the 22-month-old mice were deaf for the tested frequencies (data not shown); however, balance appeared to be normal in those animals. SEM images of old mice organs of Corti showed dramatic loss of OHCs, whereas IHCs appeared to be mostly preserved (Fig. 4a). In contrast, SEM of vestibular organs did not show HC loss in the sensory epithelium, although the stereocilia seemed to be thicker than younger ones (Fig. 4b). Most of the OHC stereocilia were shorter or missing, suggesting that the cells would eventually die as a consequence of loss-of-function (Fig. 4c). IHCs exhibited disorganized bundles and bulgy surfaces (Fig. 4d), while the stereocilia often appeared longer, thicker and fused (Figs. 4d and e). The fact the stereocilia was longer than normal ones indicated that the actin treadmilling mechanism became unbalanced during aging.

Immunogold labeling revealed that both isoforms were present at the same regions described earlier for the younger animals (Figs. 4f-g for β-actin and Figs. 2h-i for γ-actin); however, the ratio between both isoforms changed dramatically. According to the gold-particle quantification, the amount of γ-actin clearly decreased in all the analyzed compartments of vestibular hair cells. The ratio of γ- to β-actin in stereocilia dropped almost 70%; while in the cuticular plate and junctional area the ratios were even lower (Table 3). These data suggest that γ-actin expression is highly decreased during the aging process; or β-actin expression is increased at least in vestibular HCs. The gold-particle quantification of cochlear HCs was not shown due to the very low number of cells found in the old mice as observed in SEM images.

Discussion

The immunogold labeling is a technique that provides primarily the molecular localization at the electron microscopy level. Several authors have taken advantage of this method for the precise location of important proteins involved in hearing or balance functions (Rzadzinska et al., 2004; Kazmierczak et al., 2007; Mahendrasingam et al., 2010; Pepermans et al., 2014). Gold-particle quantification is a useful tool to provide evidence about the relative amounts of certain proteins (Bergersen et al., 2008; D'Amico and Skarmoutsou, 2008; Xie et al., 2010; Mayhew 2011). However, post-embedding gold labeling has limitations. It is a fact that the chemical fixation attenuates the epitope signal. The use of a mild fixation followed by cryoimmobilization, freeze-substitution, and acrylic resin embedding improve the preservation of the available epitopes. Post-embedding does not reveal the absolute amounts of the studied molecule(s). Also, one cannot guarantee that the primary antibodies will recognize all the available epitopes on the ultrathin section. In this paper, it was intended to obtain the most precise methodological approach for the actin isoform quantification and to provide new piece of evidence about actin turnover in inner ear hair cells.

The data obtained here by immunogold of the two cytoplasmic actin isoforms suggest that HCs can control the proportions of actin isoforms throughout its lifetime. In other words, the actin-based structures such as stereocilia, cuticular plates, and adherens junctions seem to be dynamically turned over when comparing the actin-labeling in embryonic, adult and old stages. There was a trend in which γ-actin was higher in early stages of the HC development and progressively declined during aging (at least in vestibular HCs). Instead, another less probable possibility is that β-actin expression could increase. An interesting finding was that the stereocilia morphology of OHC observed in aged mice resembled the stereocilia of 16-week-old, γ-actin KO mice (Belyantseva et al., 2009), suggesting that the lack of or decreasing of γ-actin could profoundly affect the stereocilia function during the aging process.

Little is known about the contribution of each isoform in the polymerization and depolymerization of the actin structures in different cell types. Cellular actin formations can be static or dynamic, and the proportions of the isoforms might play a key role in filament stiffness and plasticity. New technologies such as gene-vector transfections and Cre-lox have been shedding light on the comprehension of the cytoplasmic actin isoform functions (Bunnell and Ervasti, 2011). In myoblasts, the overexpression of β-actin increased the migration speed and the number of membrane projections (Peckham, 2001). Instead, Simiczyjew et al. (2014), while studying human colon cancer cells, observed that the migration speed in vitro was significantly higher in cells overexpressing γ-actin. Bergeron et al. (2010) tested in vitro the formation of polymers of both isoforms (isolated or combined) in the presence of Ca or Mg ions, and verified that during the heteropolymeric filament formation, the presence of Ca-γ-actin may delay the equilibrium between globular and filamentous forms, causing a slower polymerizing actin with greater filament stability. Calcium inflow occurs in stereocilia when electromechanical-gated channels open during signal transduction. This produces a local concentration that could affect the actin dynamics in developing and mature cells. The actin turnover in microvilli in intestinal cells is faster than in stereocilia because the intestinal cells are in constant renewal and must reach adulthood faster than HCs (Stidwill et al., 1984). Slower actin polymerization is expected in HCs because the hair bundle deflection after a mechanical stimulation is in the nanometric scale, and the actin core needs to be steady enough to perceive this displacement.

Early studies from Schneider et al. (2002) and Rzadzinska et al. (2004) indicated that the stereocilia actin core undergoes constant rebuilding, with polymerization at the barbed ends of the actin filaments (at stereocilia tips) and a matched depolymerization at the pointed ends (at the stereocilia base). The resultant flux of actin from the tip to the base was similar to, albeit much slower than, the actin recycling and treadmilling described in other actin protrusions, such as those at the leading edge of cells (Le Clainche et al., 2008). An extraordinary feature of this self-renewal is that the flux rates are proportional to the length of the stereocilia and inversely related to the age of the stereocilia (Schneider et al., 2002; Rzadzinska et al., 2004), suggesting that the mechanisms for length regulation and self-renewal of the actin core are integrated. Zhang and coworkers in 2012 have shown a different perspective on actin turnover in adult hair cell stereocilia. They showed that in adult frogs and mice, and in neonatal mice (in vivo and in vitro), the stereocilia were remarkably stable, incorporating newly synthesized protein at <10% per day. Also, the

authors noticed that only the stereocilia tips presented a rapid turnover, discarding the treadmilling as the mechanism of protein incorporation along the whole stereocilia core. Based on the fluctuations of actin isoforms, the treadmilling explanation is more plausible for the stereocilia physiology. It is very unlikely that highly active cells such as the HCs, restrict the incorporation of newly stereocilia protein to the tip only.

In animal models, Actg KO mice exhibit hearing loss at very early stages of development, which suggest critical and specific functions for γ-actin in HCs (Belyantseva et al., 2009). Perrin and co-workers (2010) demonstrated that Actg1-flox Atoh1-cre mice have nearly normal hearing as young adults, but later develop progressive hearing loss at all frequencies tested. According to the quantitative immunogold labeling shown here, γ-actin was the prominent isoform in E16.5, whereas in adulthood the isoforms appeared in equal amounts. In two-year-old mice, the amount of γ-actin in vestibular HC was dramatically reduced when compared with β-actin. Perhaps this decrease also occurs in cochlear HC and could be related to stereocilia modifications and concomitant progressive hearing loss in aging animals, as pointed out by γ-actin mutant mice (Belyantseva et al. 2009). Yet, point mutations on chromosome 17q25.3 in ACTG1 gene in humans cause autosomal dominant progressive sensorineural hearing loss (DFNA20/26) (Morel et al., 2000; DeWan et al., 2003; Van Wijk et al., 2003; Rendtorff et al., 2006). All the patients have in common an early and progressive sensorineural hearing loss, but the mechanism which γ-actin acts is unknown. According to this paper, one possibility that should be explored in future studies of DFNA20/26 is the decrease of the total γ-actin concentrations. This might affect hair cell functions and give rise to the onset of deafness observed in humans.

The results shown here suggest that the HC might control the expressions of the actin isoform during embryonic, post-natal development and mature stages. This shift in isoform proportions may modulate the affinity of actin filaments for different actin binding proteins, as well as stereocilia stiffness and speed of polymerization. Actin monomers are peripherally transported towards the stereocilia tips through a narrow annular space between the plasma membrane and the actin shaft. Actin labeling at the periphery of the adult stereocilia was observed, indicating that actin monomers were likely moving themselves up and down between the membrane and the actin shaft. Most monomers are incorporated into the actin core after reaching the stereocilia tips, because of the small and confined space (Schneider et al., 2002). As pointed out by the immunogold quantification, the concentration of both isoforms was similar in adult stereocilia. However, γ-actin was much higher in the cuticular plate and junctions suggesting that actin filaments rich in γ-actin monomers were more stable and stiffer, as needed in stereocilia.

These proportions might be maintained until the HCs start to age. During the aging process, the OHCs located at the basal turn senesce and die earlier than mid-apical OHCs. It was observed that OHC stereocilia progressively degenerate and this might be the trigger for the cell death, per se. On the other hand, the IHCs survive, but their stereocilia are no longer functional as shown by the ABR tests. Disorganizing bundles with loss of the staircase, fused and long stereocilia were observed. Even considering that aging alters the normal metabolism, the extremely long stereocilia in the two-year old IHCs indicate that actin incorporation persists even after the stereocilia reach maturity. More investigation needs be

done to determine if the unbalance of the actin isoforms is one of the triggers for the stereocilia disorganization and subsequent cell death.

Overall, the data presented here provided evidence for continuous plasticity of the actin-based structures present in HCs, with an apparent age-related reduction in capacity for renewal of γ-actin.

Materials and Methods

Animals

All animals used in this work were handled following the NIH Guidelines for Animal Care and approved by NIDCD Animal Protocol Committee (#1215-08). For the immunogold labeling studies, 2 pregnant mice at the embryonic stage 16.5 (E16.5), 3 post-natal day 4 mice (P4), 3 eight-week-old mice, 3 22-month-old mice were used (all mice C57BL/6J strain). Yet, 2 three-month-old guinea pigs (*Cavia porcellus*), 2 two-month-old bullfrogs (*Rana catesbeiana*), 2 post-natal day 1 (P1) chicks (*Gallus gallus*) for immunoEM (antibody specificity tests), 3 eight-week-old rats (Sprague Dawley strain) were used for immunofluorescence, and 3 22-month-old mice were used for hearing test and SEM. Fixed inner ears from 2 Actg1$^{-/-}$ mice were kindly provided by Dr. James Ervasti (University of Minnesota) and used as the negative control for γ-actin antibody.

Antibodies

Mouse monoclonal anti-β-Actin was obtained from Sigma-Aldrich (Clone AC-74, Catalog# A2228) and it recognizes an epitope located on the N-terminal end of the β-isoform of actin. Product data-sheet indicates that BALB/c mice were immunized with the synthetic β-cytoplasmic actin N-terminal peptide acetyl-DDDIAALVIDDGSGK conjugated to keyhole limpet hemocyanin (KLH), and then affinity-purified. Mouse monoclonal anti-γ-actin was obtained from Santa Cruz Biotechnology Inc. (1-24, Catalog# sc-65635) and it also recognizes an epitope located on the unique N-terminal. The synthetic peptide acetyl-EEEIAALVIDDGSGC coupled with KLH was injected in mice and affinity-purified against immobilized bovine brain γ-actin. Goat anti-mouse IgG coupled with Alexa 488 (Invitrogen) was used for immunofluorescence. Rabbit anti-mouse IgG (BBInternational) coupled with 10 nm gold particles was used for immunoEM.

Immunofluorescence

Eight weeks old adult rats (N=3) with were euthanized in a CO_2 chamber and decapitated. Their inner ears were then removed and immediately immersed in a fixative solution containing 2% formaldehyde in 0.1 M sodium phosphate saline (PBS) for 20 min at room temperature (RT). After fixation, samples were washed in PBS 3 × 10 min, permeabilized with 0.5% Triton X-100 for 10 min, blocked overnight with 4% bovine albumin in PBS at 4°C, incubated with primary antibodies for 2 h RT, washed 3 X 10 min in PBS, incubated with secondary fluorescent antibody for 1 h RT, washed 3 × 10 min in PBS, counterstained with phalloidin-Alexa Fluor 568 (Invitrogen), and transferred to glass slides with antifade mounting medium (Prolong Gold, Invitrogen). Samples were observed in a laser-scanning microscope Zeiss 710 and a spinning disk confocal microscope Nikon Ti-E.

Sample preparation for TEM

Two pregnant (for E16.5, N=6, 3 of each female), P4 (N=3, two different litters), adult (N=3, 2 different litters) and old (N=3, 3 different litters) mice were euthanized in a CO_2 chamber and decapitated. Embryos were immediately removed after an abdominal incision and the heads immersed in fixative (described below). The inner ears were removed in P4, adult, and old mice, and immersed in fixative containing 4% formaldehyde (EMS), 0.25% glutaraldehyde (EMS), 50 mM Hepes buffer (Sigma), 2 mM $CaCl_2$, 1 mM $MgCl_2$ and 140 mM NaCl for 2 h RT. After 3 washes of 10 min in the same buffer, the tissues were cryoprotected with graded glycerol baths (10%, 20%, 30%) and plunge-frozen into liquid Freon 22 cooled by liquid nitrogen. The samples were freeze-substituted with 1.5% uranyl acetate (Ted Pella) in anhydrous methanol (Merck) for 24 h at -90°C (Leica AFS machine), embedded in the Lowicryl acrylic resin (EMS) and polymerized at -45°C for 4 days under UV light.

All the specimens were prepared as identically as possible to avoid intrinsic methodological variations for the fixation and post-embedding immunolabeling. The embryos and P4 mice were dissected and fixed in the same fixative solution on one day, while adults and old mice were prepared the next day. All fixed inner ear patches obtained from the different animals were cryoprotected and plunge-frozen on the same day. Then, the samples were freeze-substituted in one round to equalize the conditions. The other animals (frogs, guinea pigs and chicks) were dissected, fixed and freeze-substituted on different days.

Immunogold labeling

The resin blocks were trimmed and ultrathin sections (70 nm) were obtained with a new diamond knife (Diatome) in an ultramicrotome (Leica Ultracut). Sections were placed onto nickel grids (300-mesh thin-bar, EMS) treated with Grid Coat Pen (EMS) (intended to a better adhesion of the sections). Grids with sections were placed on plastic plate stands (Hiraoka staining kit, NEM, Japan) (intended to avoid heavier gold clusters to precipitate on the sections), and a solution containing 50 mM glycine (Fisher Scientific) (intended to block free aldehyde residues), 0.1% sodium borohydride (Sigma-Aldrich) (intended to dissolve slightly the resin and unmask the epitopes), and 100 mM Tris buffer saline (TBS) (intended to block free aldehyde residues) was kept for 5 min at room temperature. The sections were treated with 10% normal goat serum (NGS) (Aurium) (intended to block unspecific reacting sites) for 1 h, incubated with primary antibodies (1 μg/mL) for 2 h RT, washed 3 × 10 min with 1% NGS/TBS, incubated with the secondary antibody gold-tagged for 1 h RT, washed 3 × 10 min in TBS and finally 3 × 10 min with distilled water. Sections were stained with aqueous 1% uranyl acetate for 15 min and observed in a JEOL 1010, operated at 80 kV. Digital images were acquired using a CCD camera (AMT, Woburn, MA) at 2048 × 2048 pixels of resolution.

A total of 31 independent rounds of incubations were realized for this paper as follows: 17 repetitions for E16.5, P4, adult, and old mice; 5 repetitions for chicks, frogs and guinea pigs; 5 for fluorescence; and 4 for $Actg1^{-/-}$ mice. A minimum of three grids with at least four sections for each time/animal was used for each round of incubation.

Gold-particle quantification

Gold particles from both isoform labeling were quantified in HC stereocilia, cuticular plates and adherens junctions of mice in three different stages: E16.5, adults and old mice. The original scale bars from the TEM images were used to calibrate the program ImageJ (NIH) for the gold measures. In each image, the threshold level was adjusted to highlight the gold-particles from the background. Then, regions of interest were manually contoured and the "analyze particle" function used to count the number of gold-particles per square-micron (gold/μm^2). The statistical analysis of the differences between actin isoform gold-particles in the cited hair cell compartments was measured by analysis of variance (ANOVA) and Bonferroni's post hoc test. The level of significance was set at 10%.

A total of 533 images were taken for the gold particle quantification. A minimum of 11 different hair cells (cochlear or vestibular) for each one of the 3 different animals for the three ages was used for the quantification. The total of number of gold particles distributed in the total area (μm^2) measured in the electronmicrographs is shown in Table 1.

Scanning electron microscopy

Organs of Corti from the three 22-month-old mice tested for hearing were fixed with 4% formaldehyde, 2.5% glutaraldehyde, 50 mM Hepes buffer, 2 mM $CaCl_2$, 1 mM $MgCl_2$ and 140 mM NaCl for 2 h RT. Samples were prepared by OTOT method where two consecutive baths of 1% osmium tetroxide (EMS) and 1% tannic acid (Sigma-Aldrich) are applied for 1 h with 3 × 10 min washes in between. Then the samples were dehydrated in a graded series of ethanol till absolute, critical-point dried (Baltec CPD 050), placed on aluminum stubs and observed in a cold field emission SEM (Hitachi S4700), operated at 5 kV.

Supplementary Material

Refer to Web version on PubMed Central for supplementary material.

Acknowledgments

I would like to thank Dr. Bechara Kachar (NIDCD, NIH) for the laboratorial support, Dr. Ronald Petralia (NIDCD, NIH) for the use of the TEM, Dr. M'hamed Grati (UM, FL), Dr. Felipe Salles (Stanford University) and Dr. Uri Manor (NIH, MD) for the critical and useful discussions, and Nicole Thompson (NIDCD, NIH) for the grammar correction. I declare no conflict of interest.

Abbreviations

β-	beta
γ-	gamma
HCs	hair cells
OHC	outer hair cell
IHC	inner hair cell
ABR	auditory brainstem responses

References

Belyantseva IA, Perrin BJ, Sonnemann KJ, Zhu M, Stepanyan R, McGee J, Frolenkov GI, Walsh EJ, Friderici KH, Friedman TB, et al. Gamma-actin is required for cytoskeletal maintenance but not development. Proc. Natl. Acad. Sci. USA. 2009; 106:9703–9708. [PubMed: 19497859]

Bergeron SE, Zhu M, Thiem SM, Friderici KH, Rubenstein PA. Ion dependent polymerization differences between mammalian beta- and gamma non muscle actin isoforms. J. Biol. Chem. 2010; 285:16087–16095. [PubMed: 20308063]

Bergersen LH, Storm-Mathisen J, Gundersen V. Immunogold quantification of amino acids and proteins in complex subcellular compartments. Nat. Protoc. 2008; 3(1):144–52. [PubMed: 18193031]

Bunnell TM, Ervasti JM. Structural and Functional Properties of the Actin Gene Family. Critical Reviews in Eukaryotic Gene Expression. 2011; 21(3):255–266. [PubMed: 22111713]

D'Amico F, Skarmoutsou E. Quantifying immunogold labelling in transmission electron microscopy. J. Microsc. 2008; 230(1):9–15. [PubMed: 18387034]

DeWan AT, Parrado AR, Leal SM. A second kindred linked to DFNA20 (17q25.3) reduces the genetic interval. Clin. Genet. 2003; 63:39–45. [PubMed: 12519370]

Dugina V, Zwaenepoel I, Gabbiani G, Clement S, Chaponnier C. Beta-and gamma-cytoplasmic actins display distinct distribution and functional diversity. J. Cell. Sci. 2009; 122:2980–2988. [PubMed: 19638415]

Furness DN, Katori Y, Mahendrasingam S, Hackney CM. Differential distribution of beta- and gamma-actin in guinea-pig cochlear sensory and supporting cells. Hear. Res. 2005; 207:22–34. [PubMed: 16024192]

Hofer D, Ness W, Drenckhahn D. Sorting of actin isoforms in chicken auditory hair cells. J. Cell. Sci. 1997; 110:765–770. [PubMed: 9099950]

Kazmierczak P, Sakaguchi H, Tokita J, Wilson-Kubalek EM, Milligan RA, Muller U, Kachar B. Cadherin 23 and protocadherin 15 interact to form tip-link filaments in sensory hair cells. Nature. 2007; 449(6):87–92. [PubMed: 17805295]

Le Clainche C, Carlier MF. Regulation of actin assembly associated with protrusion and adhesion in cell migration. Physiol. Rev. 2008; 88:489–513. [PubMed: 18391171]

Mahendrasingam S, Beurg M, Fettiplace R, Hackney CM. The ultrastructural distribution of prestin in outer hair cells: a post-embedding immunogold investigation of low and high frequency regions of the rat cochlea. Eur. J. Neurosci. 2010; 31(9):1595–1605. [PubMed: 20525072]

Mayhew TM. Quantifying immunogold localization on electron microscopic thin sections: a compendium of new approaches for plant cell biologists. J. Exp. Bot. 2011; 62(12):4101–13. [PubMed: 21633081]

Morell RJ, Friderici KH, Wei S, Elfenbein JL, Friedman TB, et al. A new locus for late-onset, progressive, hereditary hearing loss DFNA20 maps to 17q25. Genomics. 2000; 63:1–6. [PubMed: 10662538]

Morín M, Bryan KE, Mayo-Merino F, Goodyear R, Mencía A, Modamio-Høybjør S, del Castillo I, Cabalka JM, Richardson G, Moreno F, et al. In vivo and in vitro effects of two novel gamma-actin (ACTG1) mutations that cause DFNA20/26 hearing impairment. Hum. Mol. Genet. 2009; 18(16): 3075–3089. [PubMed: 19477959]

Peckham M, Miller G, Wells C, Zicha D, Dunn GA. Specific changes to the mechanism of cell locomotion induced by overexpression of beta-actin. J. Cell Sci. 2001; 114:1367–77. [PubMed: 11257002]

Pepermans E, Michel V, Goodyear R, Bonnet C, Abdi S, Dupont T, Gherbi S, Holder M, Makrelouf M, Hardelin J, et al. The CD2 isoform of protocadherin-15 is an essential component of the tip-link complex in mature auditory hair cells. EMBO Mol. Med. 2014; 6(7):984–992. [PubMed: 24940003]

Perrin BJ, Sonnemann KJ, Ervasti JM. β-actin and γ-actin are each dispensable for auditory hair cell development but required for Stereocilia maintenance. PLoS Genet. 2010; 6(10):e1001158. [PubMed: 20976199]

Procaccio V, Salazar G, Ono S, Styers ML, Gearing M, Davila A, Jimenez R, Juncos J, Gutekunst CA, Meroni G, Fontanella B, Sontag E, Sontag JM, Faundez V, Wainer BH. A mutation of beta-actin that alters depolymerization dynamics is associated with autosomal dominant developmental malformations, deafness, and dystonia. Am. J. Hum. Genet. 2006; 78:947–960. [PubMed: 16685646]

Rendtorff ND, Zhu M, Fagerheim T, Antal TL, Jones M, Teslovich TM, Gillanders EM, Barmada M, Teig E, Trent JM, et al. A novel missense mutation in ACTG1 causes dominant deafness in a Norwegian DFNA20/26 family, but ACTG1 mutations are not frequent among families with hereditary hearing impairment. Eur. J. Hum. Genet. 2006; 14:1097–1105. [PubMed: 16773128]

Rzadzinska AK, Schneider ME, Davies C, Riordan GP, Kachar B. An actin molecular treadmill and myosins maintain stereocilia functional architecture and self-renewal. J. Cell Biol. 2004; 164(6): 887–897. [PubMed: 15024034]

Schneider ME, Belyantseva IA, Azevedo RB, Kachar B. Rapid renewal of auditory hair bundles. Nature. 2002; 418:837–838. [PubMed: 12192399]

Schwander M, Kachar B, Muller U. The cell biology of hearing. J. Cell Biol. 2010; 190(1):9–20. [PubMed: 20624897]

Shawlot W, Deng JM, Fohn LE, Behringer RR. Restricted betagalactosidase expression of a hygromycin-lacZ gene targeted to the beta-actin locus and embryonic lethality of beta-actin mutant mice. Transgenic Res. 1998; 7:95–103. [PubMed: 9608737]

Simiczyjew A, Antonina JM, Popow-Wozniak A, Malicka-Błaszkiewicz M, Nowak D. Effect of overexpression of β- and γ-actin isoforms on actin cytoskeleton organization and migration of human colon cancer cells. Histochem. Cell. Biol. 2014; 142:307–322. [PubMed: 24682235]

Slepecky N, Chamberlain SC. Immunoelectron microscopic and immunofluorescent localization of cytoskeletal and muscle-like contractile proteins in inner ear sensory hair cells. Hear. Res. 1985; 20(3):245–60. [PubMed: 3910630]

Stidwill RP, Wysolmerski T, Burgess DR. The brush border cytoskeleton is not static: in vivo turnover of proteins. J. Cell Biol. 1984; 98:641–645. [PubMed: 6693500]

Tilney LG, Tilney MS, DeRosier DJ. Actin filaments, stereocilia, and hair cells: how cells count and measure. Annu. Rev. Cell Biol. 1992; 8:257–74. [PubMed: 1476800]

Vandekerckhove J, Weber K. At least six different actins are expressed in a higher mammal: an analysis based on the amino acid sequence of the amino-terminaltrypticpeptide. J. Mol. Biol. 1978; 126:783–802. [PubMed: 745245]

van Wijk E, Krieger E, Kemperman MH, De Leenheer EM, Huygen PL, Cremers CW, Cremers FP, Kremer H. A mutation in the gamma actin 1 (ACTG1) gene causes autosomal dominant hearing loss (DFNA20/26). J. Med. Genet. 2003; 40:879–884. [PubMed: 14684684]

Xie L, Hoffert JD, Chou CL, Yu MJ, Pisitkun T, Knepper MA, Fenton RA. Quantitative analysis of aquaporin-2 phosphorylation. Am. J. Physiol. Renal Physiol. 2010; 298(4):F1018–23. [PubMed: 20089674]

Weaver SP, Hoffpauir J, Schweitzer L. Actin distribution along the lateral wall of gerbil outer hair cells. Brain Res. Bull. 1993; 31(1-2):225–8. [PubMed: 8453489]

Zhang D, Piazza V, Perrin BJ, Rzadzinska AK, Poczatek JC, Wang M, Prosser HM, Ervasti JM, Corey DP, Lechene CP. Multi-isotope imaging mass spectrometry reveals slow protein turnover in hair-cell stereocilia. Nature. 2012; 481:520–524. [PubMed: 22246323]

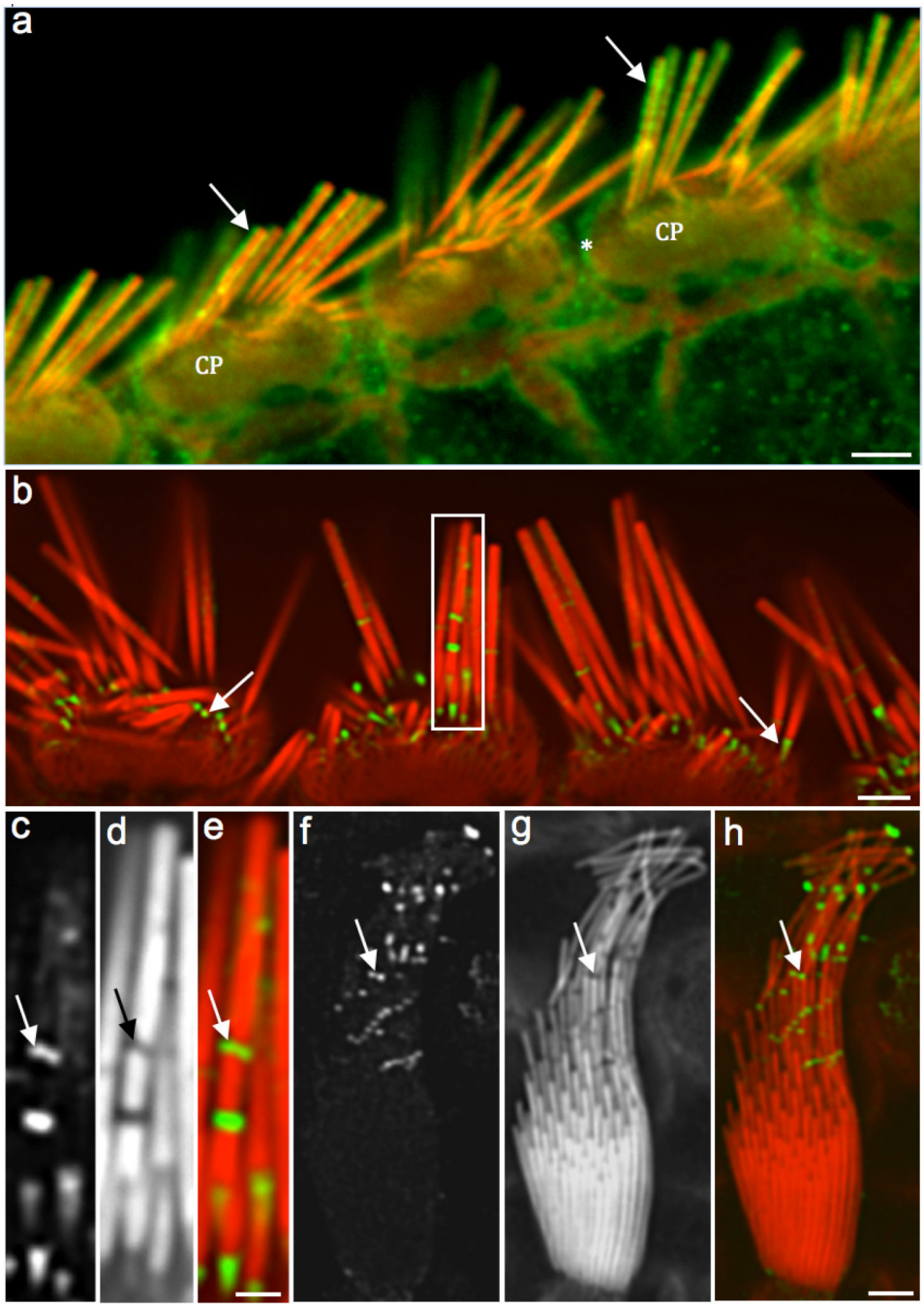

Figure 1. Immunofluorescence shows a weak penetration of γ-actin antibody into the stereocilia shaft

Fig. 1a: Confocal microscopy image of adult rat IHCs showing the γ- actin labeling (green) at the stereocilia periphery (arrows), cuticular plates (CP) and junctional complex (*). Fig. 1b: Another adult rat organ of Corti with γ-actin labeling (green) with emphasis on the concentrated signals along and at the base of the stereocilia (arrows). Figs. 1c (γ-actin label), 1d (phalloidin) and 1e (composite) images (white rectangle in Fig. 1b) show a high magnification of the labeling into the stereocilia gaps (arrows). Figs. 1f (γ-actin labeling), 1g (phalloidin), and 1h (composite) show a rat utricle HC with concentrated fluorescence

signals where the stereocilia bent (arrows). Absence of phalloidin labeling indicates the presence of actin monomers and not actin filaments within these gaps. Scale bars: 1a and 1b = 2 μm; 1c-e = 200 nm; 1f-h = 0.5 μm

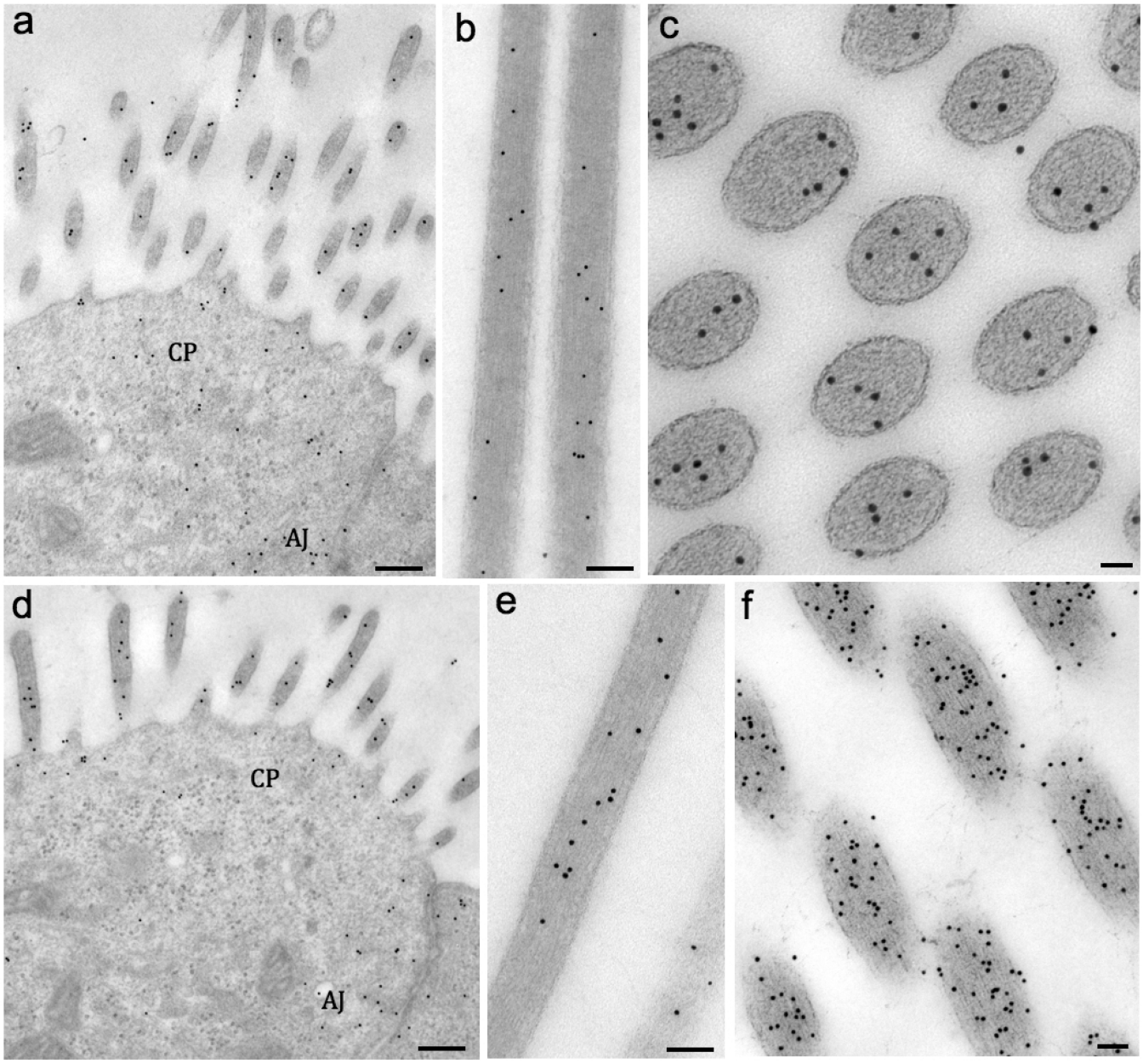

Figure 2. Immunogold labeling reveals β- and γ-actin as early as E16.5 mouse in all actin-based structures

Fig. 2a: TEM image of cochlear OHCs showing the gold-particles labeling β-actin in stereocilia, cuticular plate (CP) area and adherens junctions (AJ). The same locations were labeled for γ-actin as shown in Fig. 2d. Fig. 2b: Utricle stereocilia longitudinally sectioned and labeled for β-actin. Fig. 2c: Tangential section of semicircular canal crista stereocilia labeled for β-actin. Fig 2e: Utricle stereocilia longitudinally sectioned and labeled for γ-actin.Fig. 2f: Tangential section of crista stereocilia labeled for γ-actin. Scale bars: 2a and d = 1 μm; 2b, c, e and f = 50 nm

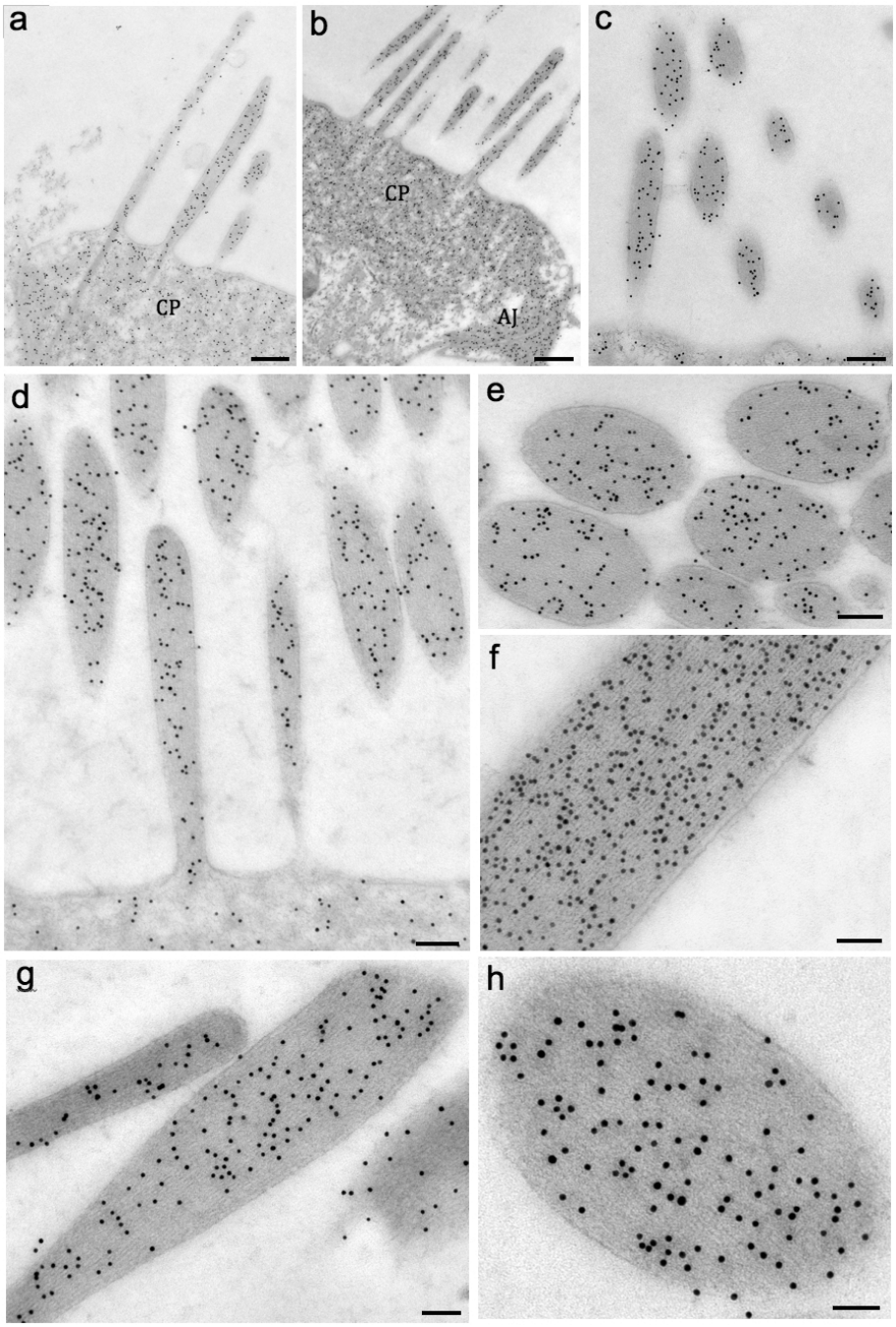

Figure 3. β- and γ-actin seems to be equally expressed in adult hair cell stereocilia

Fig. 3a (β-actin) and Fig. 3b-c (γ-actin) show the colocalization of both isoforms in stereocilia, cuticular plate (CP), and adherens junctions (AJ) of P4 mouse cochlea HC. Figs. 3d-f show the γ-actin gold-particle distribution in stereocilia. Figs. 3g and h show the labeling for β-actin. Scale bars: 1a and 1b = 0.5 μm; 1c = 150 nm; 1d, 1e and f = 100 nm; 1g = 100 nm; 1h = 50 nm

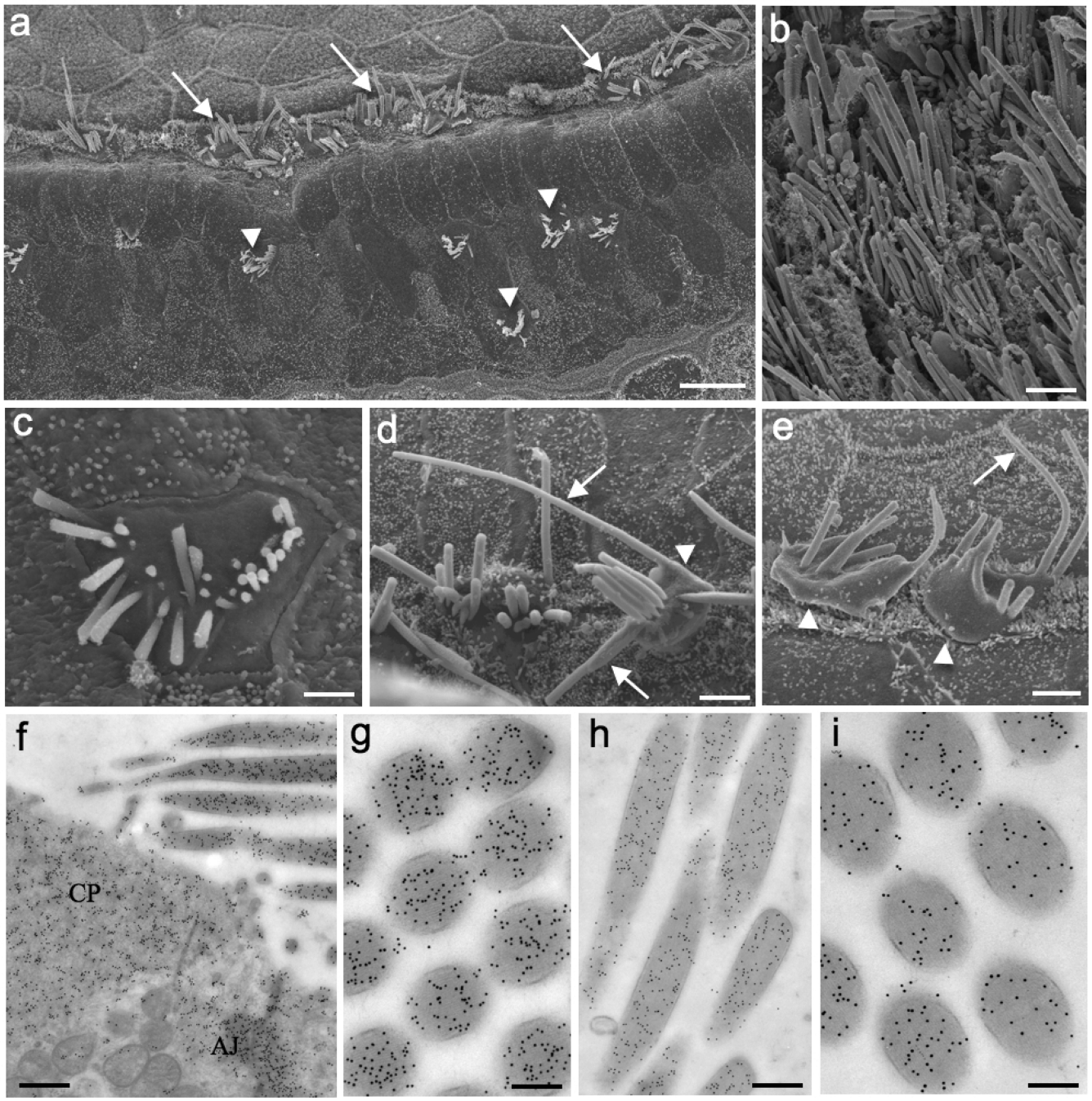

Figure 4. The γ to γ-actin ratio changes considerably in aged mice

Fig. 4a: SEM image of old mouse organ of Corti showing altered IHCs (arrows) and few remaining OHCs (arrowheads) in the three rows of the sensory epithelium. Fig. 4b: SEM of utricle displaying the HC of the sensory epithelium. Fig. 4c: SEM of an OHC surface with shorter or missing stereocilia. Figs. 4d and e: SEM of IHCs exhibiting disorganized bundles, bulgy surfaces (arrowheads) and longer stereocilia (arrows). Figs. 4f and g (β- actin)and Figs. 2h and i (γ-actin) show immunogold labeling in the same regions described for the

younger animals. Cuticular plate (CP), adherens junctions (AJ). Scale bars: 1a = 100 μm; 1b = 5 μm; 1c = 3 μm, 1d and e = 5 μm; 1f = 150 nm; 1g and i = 150 nm; h = 300 nm

Table 1

Absolute numbers of gold particles counted in the area measured (in μm^2) for the immunogold labeling quantification for each actin isoform and the different ages of the cochlear and vestibular hair cells.

Gold particles I total area	Cochlear HCs	Vestibular HCs
E16.5 Beta	716 / 21.5	856 / 36.5
E16.5 Gamma	950 / 21.6	1,264 / 39.7
Adult Beta	10,603 / 88	12,893 / 146
Adult Gamma	23,864 / 128	25,047 / 177
Old Beta	-	31,466 / 226
Old Gamma	-	11,847 / 316

Table 2

Gold particle quantification of the two actin isoforms found in different cochlear hair cell compartments in different ages.

Cochlear Hair Cells	Stereocilia	Cuticular plates	Junctions
Gamma (E16.5)	176 ± 49	25 ± 11	146 ± 39
Beta (E16.5)	125 ± 32	27 ± 14	94.6 ± 18
Ratio γ/B (E16.5)	**1.4***	**0.92**	**1.55***
Gamma (Adult)	461 ± 132	101 ± 35	212 ± 71
Beta (Adult)	460 ± 154	56 ± 21	115 ± 60
Ratio γ/B (Adult)	**1.0**	**1.8***	**1.84***

The values represent the mean and standard deviation of gold-particles per μ^2. The numbers in bold represent the ratio between the isoforms.

* ratio between isoform was significantly different.

Table 3

Gold particle quantification of the two actin isoforms found in different vestibular hair cell compartments in different ages.

Vestibular Hair Cells	Stereocilia	Cuticular plates	Junctions
Gamma (E16.5)	374 ± 86	40 ± 16	146 ± 39
Beta (E16.5)	253 ± 58	42 ± 17	94.6 ± 18
Ratio γ/B (E16.5)	**1.47***	**0.95**	**1.6***
Gamma (Adult)	675 ± 245	201 ± 87	278 ± 83
Beta (Adult)	660 ± 268	96 ± 43	162 ± 81
Ratio γ/B (Adult)	**1.02**	**2.09***	**1.71***
Gamma (Old)	292 ± 64	70 ± 7	135 ± 32
Beta (Old)	801 ± 121	344 ± 69	571 ± 110
Ratio γ/B (Old)	**0.36***	**0.2***	**0.23***

The values represent the mean and standard deviation of gold-particles per μm^2. The numbers in bold represent the ratio between both isoforms.

*ratio between isoform was significantly different.